

SUPPORTING INFORMATION

Nitrogen and Sulfur Co-Doped Fluorescent Carbon Dots for Trapping of Hg(II) Ions from Water

Harpreet Kaur^a, Navneet Kaur^{*b}, Narinder Singh^{*c}

^a*Centre for Nanoscience and Nanotechnology, Panjab University, Chandigarh-160014*

^b*Department of Chemistry, Panjab University, Chandigarh-160014*

^c*Department of Chemistry, IIT Ropar, Roopnagar, Punjab-140001*

**Corresponding author (Navneet Kaur) E-mail: navneetkaur@pu.ac.in; Tel: +91-1722534405
and (Narinder Singh) E-mail: nsingh@iitrpr.ac.in; Tel: +91-1881242176.*

TABLE OF CONTENTS:

Figure S1: ESI-MS spectra of Receptor 1

Figure S2: ¹H NMR of Receptor 1

Figure S3: ¹³C NMR of Receptor 1

Figure S4: Fluorescence spectra showing stability of the CDs in the absence and presence of Hg²⁺ ions in a wide range of pH.

Figure S5: Time-dependent variation in fluorescence emission intensity of the CDs upon addition of different concentrations of Hg²⁺ ions.

Figure S6: Scanning Emission Micrographs of (A) Bare silica of mesh size 60-120, and (B) Silica coated with CDs.

Figure S7: Fluorescence emission profile of CDs upon addition of increasing concentrations of perchlorate salt.

Figure S8: Zeta Potential Report of CDs.

Figure S9: UV-Visible spectra of CDs on addition of increasing concentrations of Hg²⁺ ions (0-55 μM).

Figure S10: Fluorescence response of CDs upon addition of various anions.

Figure S11: Fluorescence emission spectra of CDs in the presence of Hg²⁺ ions in the presence of an array of anions as interferent species.

Figure S12: Cyclic Voltammogram of CDs.

Figure S13: TAUC Plot of the CDs.

Figure S14: Fluorescence emission spectra of CDs containing Hg²⁺ ions in the presence of EDTA and tetrabutylammonium hydroxide.

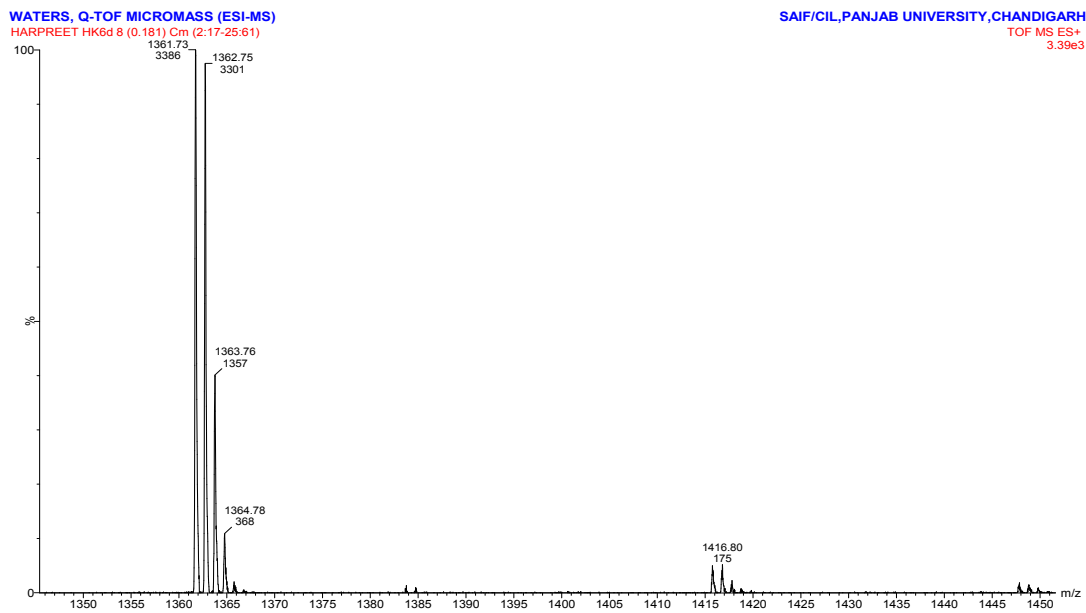


Figure S1: ESI-MS spectra of Receptor 1

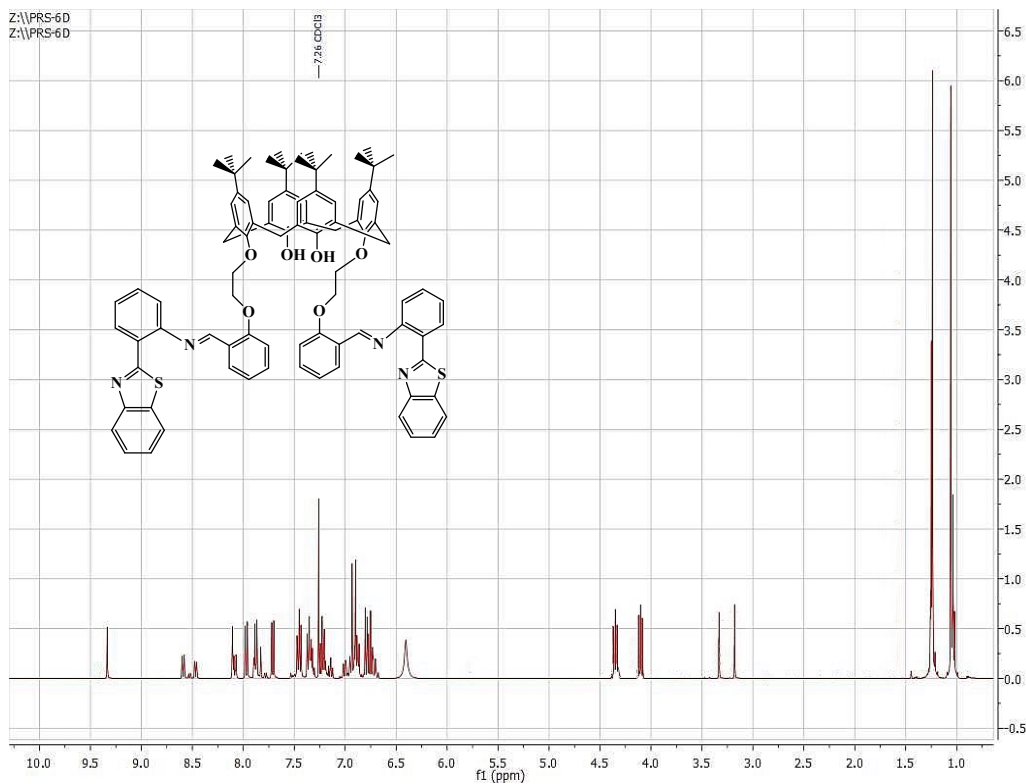


Figure S2: ¹H NMR of Receptor 1.

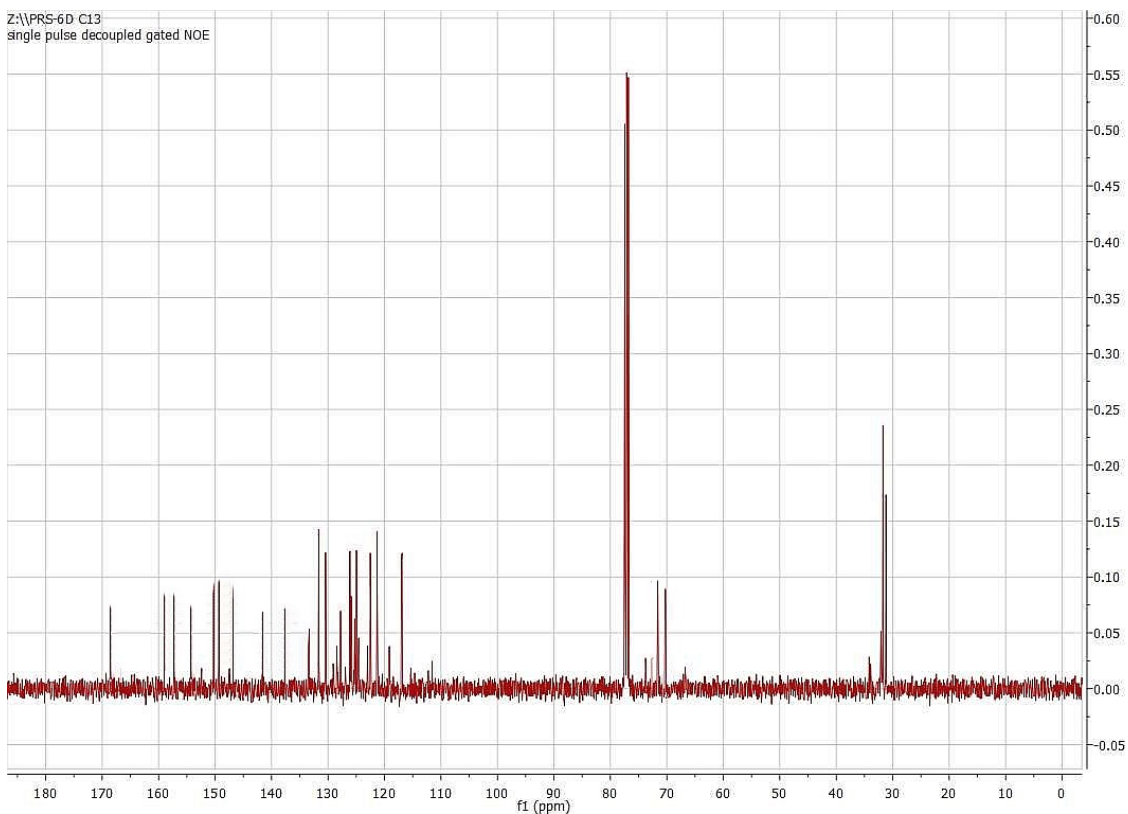


Figure S3: ^{13}C NMR of Receptor 1.

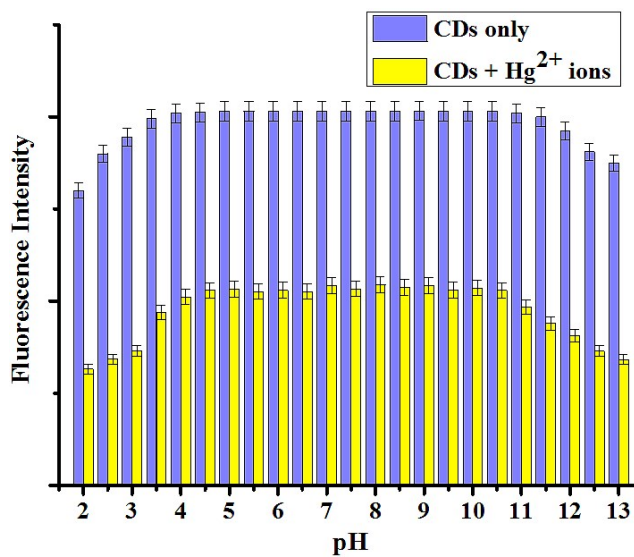


Figure S4: Fluorescence spectra showing stability of the CDs in the presence of Hg^{2+} ions in a wide range of pH.

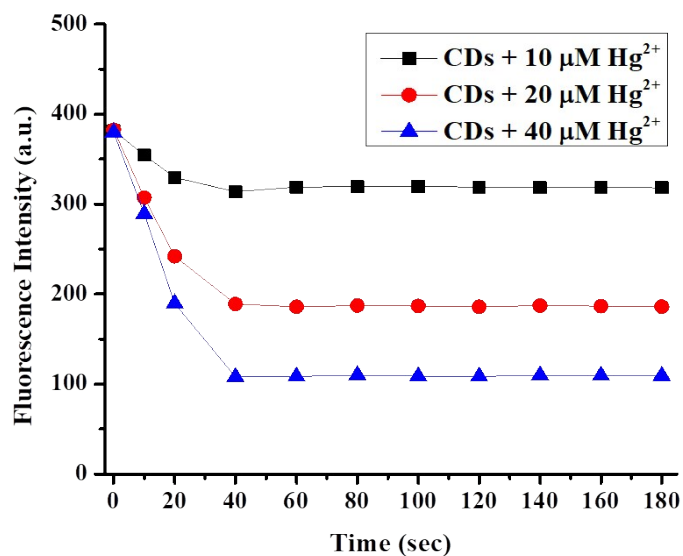


Figure S5: Time-dependent variation in fluorescence emission intensity of the CDs upon addition of different concentrations of Hg²⁺ ions (0-40 μM) showing response time of the order of less than one minute (40 secs).

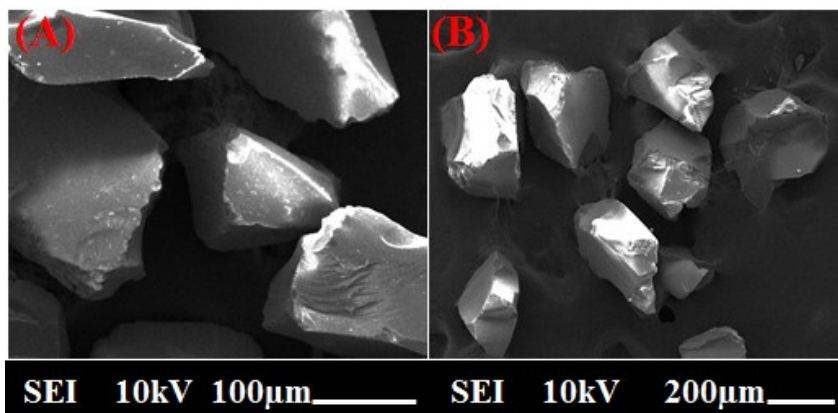


Figure S6: Scanning Emission Micrographs of (A) Bare silica of mesh size 60-120, and (B) Silica coated with CDs.

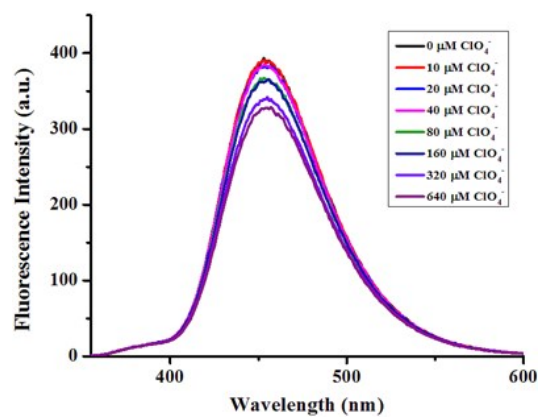


Figure S7: Fluorescence emission profile of CDs upon addition of increasing concentrations of perchlorate salt (0-640 μM).

Zeta Potential Report	
Mobility	-4.28u/s/V/cm
Zeta Potential	-54.1 mv
Charge	-0.02550 fC
Polarity	Negative
Conductivity	14 uS/cm
Field Strength	5.0 kV/m
Sample Information	
Fluid	
CDs	
Viscosity	0.81
Temperature	29.25 C
Dielectric Const	80
Dispersant	
DMSO:WATER	
pH	7
QDS	

Figure S8: Zeta Potential Report of the as-synthesized CDs.

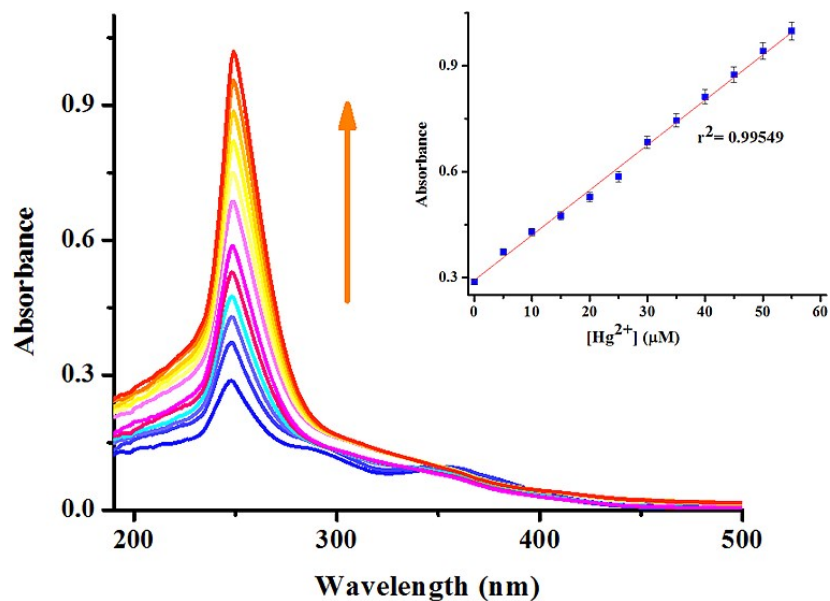


Figure S9: UV-Visible spectra of CDs on addition of increasing concentrations of Hg^{2+} ions (0-55 μM) showing hyperchromic shift in the peak at 249 nm and diminution of the peak at 350 nm with a linear progression coefficient of 0.99549 in a wide dynamic range of up to 55 μM .

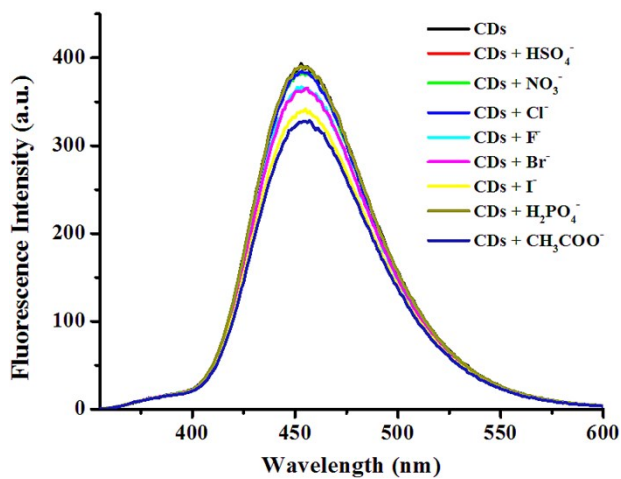


Figure S10: Fluorescence response of CDs upon addition of various anions depicting negligible change in the emission spectrum.

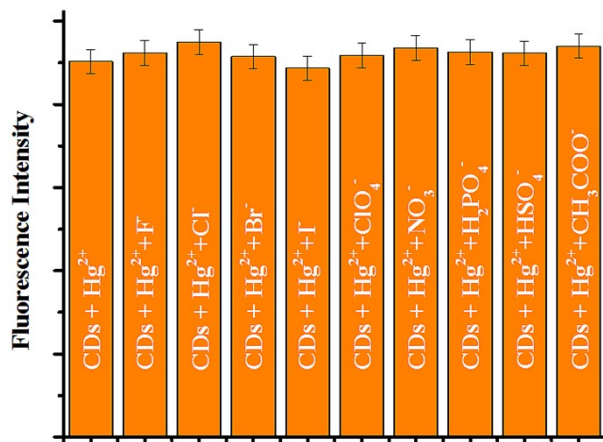


Figure S11: Fluorescence emission spectra of CDs in the presence of Hg^{2+} ions showing insignificant change upon addition of an array of anions as interferent species.

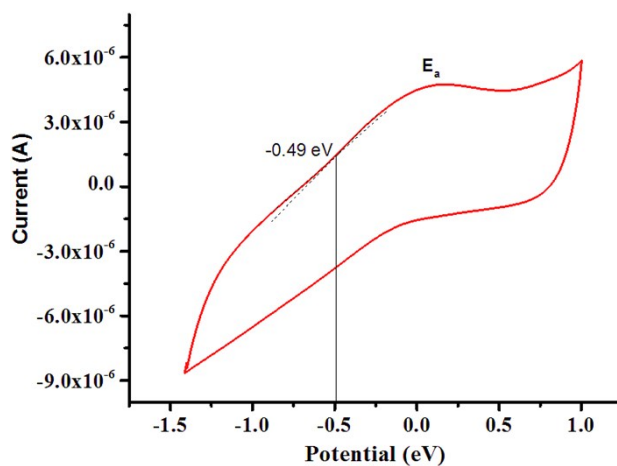


Figure S12: Cyclic Voltammogram of CDs indicating $E_{\text{ox}} = 0.49$ eV.

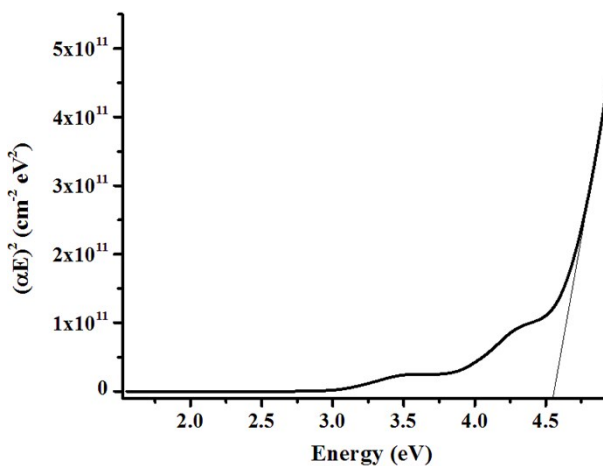


Figure S13: TAUC Plot of the CDs showing band gap of 4.55 eV.

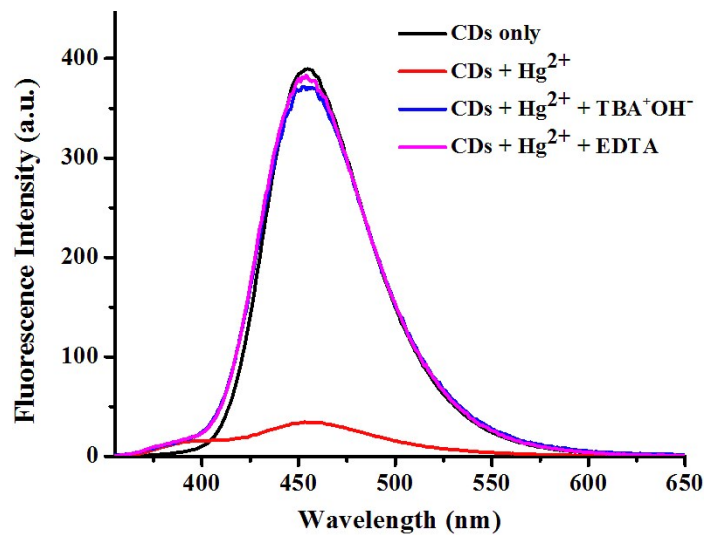


Figure S14: Fluorescence emission profile of CDs exhibits quenching in the presence of Hg²⁺ ions and the emission intensity is recovered upon addition of aqueous EDTA or tetrabutylammonium hydroxide solution.